Journal of Nuclear Medicine, published on August 25, 2016 as doi:10.2967/jnumed.115.171124

Brief Communications

In vivo Dynamic Metabolic Changes after Induced Pluripotent Stem Cells for Ischemia Injury

Shuang Wu[1-3]†, Yuankai Zhu[1-3]†, Hao Liu[1-3], Ling Tang[4,5], Ruili Du[1-3], Yehua Shen[1-3], Jin Feng[1-3], Kai Zhang[1-3], Caiyun Xu[1-3], Shouhong Zhang[1-3], Yao Chen[1-3], Fahuan Song[1-3], Yunqi Zhu[1-3], Weizhong Gu[6], Ping Ling[4,5], Ignasi Carrió[7], Hong Zhang[1-3], and Mei Tian[1-3*]

[1]Department of Nuclear Medicine and Medical PET Center, The Second Hospital of Zhejiang University School of Medicine; Hangzhou, China; [2]Institute of Nuclear Medicine and Molecular Imaging, Zhejiang University, Hangzhou, China; [3]Key Laboratory of Medical Molecular Imaging of Zhejiang Province, Hangzhou, China; [4]The First Affiliated Hospital, Zhejiang University School of Medicine, Hangzhou, China; [5]Institute of Translational Medicine, Zhejiang University, Hangzhou, China; [6]Department of Pathology, The Children's Hospital of Zhejiang University School of Medicine, Hangzhou, China; [7]Nuclear Medicine Department, Hospital Sant Pau, Autonomous University of Barcelona, Barcelona, Spain

Running title: Dynamic changes after iPSCs transplantation

Word count: 2834 words

†Contributed equally to this work.

*Corresponding author:

Mei Tian, Department of Nuclear Medicine, The Second Hospital of Zhejiang University School of Medicine, 88 Jiefang Road, Hangzhou, Zhejiang 310009, China

E-mail: meitian@zju.edu.cn

ABSTRACT

This study aims to investigate the *in vivo* dynamic metabolic changes after induced pluripotent stem cells (iPSCs) and iPSC-derived enriched cardiomyocytes (iPSC-CMs) transplantation in a rat model of cardiac ischemia injury.

Methods: Serial ^{18}F-fluorodeoxyglucose (^{18}F-FDG) positron emission tomography (PET), echocardiographic, immunohistochemical and immunofluorescent studies were performed after iPSCs and iPSC-CMs transplantation, and compared to embryonic stem cells (ESCs), ESCs-derived enriched cardiomocytes (ESC-CMs) or phosphate-buffered saline (PBS) group in rats with myocardial infarction.

Results: Increased glucose metabolism in peri-infarct areas and improved myocardial function were observed in the stem cell transplanted groups compared to the PBS control, and serial immunofluorescent and immunohistochemical results exhibited the survival and migration of stem cells during the study period.

Conclusion: Serial ^{18}F-FDG PET and echocardiographic imaging studies demonstrated the dynamic metabolic changes and myocardial functional recovery after stem cell transplantation. ^{18}F-FDG PET could be a potential approach to evaluate the *in vivo* spatiotemporal dynamic metabolic changes post iPSC or iPSC-CMs transplantation after ischemic injury.

Keywords: Positron emission tomography (PET), metabolism, myocardial ischemia, induced pluripotent stem cell (iPSC), iPSC-derived cardiomyocytes (iPSC-CMs)

INTRODUCTION

Early observations on the mechanisms of ischemic injury focused on relatively simple biochemical and physiological changes which were known to result from interruption of circulation. Subsequent research has shown molecular imaging could potentially identify pathophysiological changes *in vivo*, which is crucial for evaluating new therapeutic approaches for ischemia injury. Recently, the rapid progress of stem cell technologies has triggered an increasing interest in the use of pluripotent stem cells including embryonic stem cells (ESCs) *(1, 2)* and induced pluripotent stem cells (iPSCs) *(3, 4)* in cardiovascular ischemic repair. The new cell type, iPSCs own many similar features of ESCs, and can detour the risk of immune rejection and ethical issues. Although electrocardiographic study has found that iPSC-derived cardiomyocytes (iPSC-CMs) might be an exciting cell source for renewing myocardium *in vitro* and improving cardiac function *(5)*, to better understand the *in vivo* behavior and efficacy of iPSCs and iPSC-CMs transplantation, a noninvasive, sensitive, repeatable and quantitative imaging modality is imperative.

Since positron emission tomography (PET) can be used for both cell trafficking and therapeutic response monitoring in clinical patients, it has been referred as one of the best-suited modalities to evaluate the therapeutic effect of stem cells *(6, 7)*. Thus, we hypothesized that ^{18}F-fluorodeoxyglucose (^{18}F-FDG) PET might be useful for evaluate the spatiotemporal dynamic metabolic changes *in vivo* after transplantation of iPSCs or iPSC-CMs. To verify the above hypothesis, we performed ^{18}F-FDG micro-PET combined with echocardiography to evaluate the metabolic and functional recovery after iPSCs and iPSC-CMs transplantation in a rat model of myocardial infarction (MI), and confirmed by autoradiography (ARG), immunohistochemical and immunofluorescent analysis.

MATERIALS AND METHODS

Animal Model of MI and Stem Cell Administration

Animal model of MI was established by permanent coronary artery ligation *(8)*. Enhanced green fluorescent protein (EGFP)-labeled mouse iPSCs and ESCs, H9 human embryonic stem cells (hESCs) or induced pluripotent stem cells (hiPSCs) were cultured as described previously *(9)*. hESCs and

hiPSCs were differentiated into enriched cardiomyocytes (hESC-CMs and hiPSC-CMs) using a 2D monolayer differentiation protocol and maintained in a 5% CO_2/air environment. Details of generation of stem cells and cell culture conditions were provided in the Supplemental Materials.

To investigate the metabolic change after iPSCs transplantation, 39 adult male Sprague-Dawley rats were divided into 3 groups (n=13 per group): phosphate-buffered saline (PBS) control, mESCs or miPSCs transplantation group. Furthermore, to explore whether iPSC-CMs could improve metabolic function of injured rodent heart, additional 24 rats were divided into 3 groups (n=8 per group; all groups received tacrolimus daily): PBS control, hESC-CM or hiPSC-CM enriched group. Thirty minutes after MI, 2 X 10^6 cells were implanted by intra-myocardial injection into the peri-infarct area. Control animals received an equal volume of PBS without cells (Details were provided in the Supplementary Materials). The animal protocol has been approved by the Institutional Animal Care and Use Committee of Zhejiang University School of Medicine (Protocol No. ZJU201407-1-02-070).

^{18}F-FDG micro-PET, Echocardiography and ARG

Repeated ^{18}F-FDG micro-PET and echocardiographic studies were performed at Day 3, 7, 14, 21 and 28 after stem cell implantation. The lesion-to-normal (L/N) ratio was calculated by the following formula: L/N ratio = maximal counts per pixel of lesionregion of interest (ROI) / maximal counts per pixel of normal area *(10)*. Then the change in L/N ratio was calculated with use of the following formula: change in L/N ratio on Day N = (L/N ratio on Day N - L/N ratio on Day 3) / L/N ratio on Day 3 ×100% (N = 3, 7, 14, 21 and 28). Trans-thoracic two-dimensional and M-mode echocardiography images were obtained at the level of the papillary muscle using a Vevo 2100 system (VisualSonics Inc., Toronto, Canada). Change in left ventricular ejection fraction (LVEF) was calculated by using the following formula: change in LVEF on Day N = (LVEF on Day N - LVEF of Day 3) / LVEF on Day 3 ×100% (N= 3, 7, 14, 21 and 28). The ARG imaging was acquired after the last PET scan.

Immunohistochemical and immunofluorescent Analysis

Primary antibodies against von Willebrand factor (vWF); α-smooth muscle actin (α-SMA); cardiac

troponin I (cTNI); cardiac troponin T (cTNT) were used for immunohistochemical staining. Serial immunofluorescent analysis was processed for tracking the fate of EGFP-labeled transplanted cells at Day 3, 7, 14, 21 and 28. Cardiomyocytes, microvessels and arterioles were determined by cTNT, vWF and α-SMA, respectively.

Statistical Analysis

All data were presented as mean ± SD. One-way ANOVA test was performed to analyze the group differences, and Pearson correlation was used to examine the correlation between changes in L/N ratio and LVEF. $P < 0.05$ was considered as statistical significance.

RESULTS

Findings of micro-PET, echocardiography and ARG

Micro-PET imaging allowed the visualization of ^{18}F-FDG accumulation throughout the 28-day study period (Fig. 1A and 2A).

From Day 7-28, glucose metabolism changes (shown as Change of L/N ratio in Fig. 1B and 2B) around the peri-infarct area in both mESCs ($P < 0.05$) and miPSCs ($P < 0.05$) groups were significantly higher than that in the PBS control (Fig. 1B). The glucose metabolism increased gradually in miPSCs group at Day 21 ($P < 0.05$) and 28 ($P < 0.05$; Fig. 1B), compared to the mESCs. Similarly, in Fig. 2B, the glucose metabolism increased significantly from Day 7 to 28 in the hiPSC-CMs ($P < 0.05$) and hESC-CMs ($P < 0.05$) groups compared to the PBS group. However, no statistical difference was found between hESC-CMs and hiPSC-CMs enriched groups at Day 7, 14, 21 or 28 ($P = 0.170$, 0.421, 0.356 or 0.199, respectively).

Similarly, on echocardiographic images, myocardial function (shown as the Change of LVEF) improved significantly in the stem cell transplanted groupsfrom Day 7 to 28 after cell transplantation, compared to the PBS control group (Figs. 1C and 2C). Compared to the mESCs group, the change of LVEF was significantly lower in miPSCs group at Day 7 ($P < 0.05$), but increased gradually and became significantly higher from Day 14 to 28 ($P < 0.001$; Fig. 1D). No statistically difference was found between

hESC-CMs and hiPSC-CMs enriched groups (at Day 7, 14, 21 or 28; P = 0.087, 0.994, 0.801 or 0.492, respectively; Fig. 2D).

The micro-PET images were in agreement with the data generated from the ARG studies. During our study period, no teratoma was formed in the heart or other thoracic organs after transplantation of stem cells or stem cell-derived cardiomyocytes.

Immunohistochemical and immunofluorescent Analysis

Immunohistochemical staining demonstrated that the numbers of vWF^+ and integrated optical density (IOD) α-SMA^+ cell were significantly higher in the miPSCs or hiPSC-CMs enriched group than those in the PBS control (P < 0.05); however, no statistically significant difference was found between the miPSCs and mESCs groups, or between hiPSC-CMs and hESC-CMs enriched groups (Fig.3A-E). The IOD of cTNI or cTNT in the miPSCs or hiPSC-CMs enriched group was significantly higher than that in PBS group (P < 0.05), however, no statistically significant difference were found between the miPSCs and mESCs groups (P = 0.444) or between hiPSC-CMs and hESC-CMs enriched groups (P = 0.688).

Serial immunofluorescence studies on miPSCs, mESCs observed more $cTNT^+$ and $cTNT^+$ cells within 21 days (at Day 3, 14 to 21) compared to those at Day 28; and more vWF^+ and α-SMA^+ cells within 14 days compared to those after Day 21 (Supplemental Figs.4-8).

DISCUSSION

In this study, serial ^{18}F-FDG PET combined with echocardiographic studies demonstrated increased glucose metabolism and improved myocardial function after stem cellstransplantation compared to the PBS control. Specially, there were two important findings: (1) compared to the control group, steadily increasing of glucose metabolic recovery and functional improvement were found after iPSCs, hiPSC-CMs and hESC-CMs transplantation; (2) serial immunofluorescence and immunohistochemical results exhibited survival and migration ofstem cellswithin 28 days. To the best of our knowledge, this is the first direct comparison between miPSCs and mESCs, as well as between hESC-CMs and hiPSC-CMs in the same rat model of MI using serial ^{18}F-FDG micro-PET and echocardiographic studies,

and identified longitudinal agreement between PET imaging and immuhistochemical / immunofluorescent studies after stem cell therapy.

Selection of a better pluripotent stem cell and a more feasible noninvasive imaging technique are essentials for translating preclinical research to future clinical practice. In the past few years, the majority of studies focused on cell activities and behaviors *in vitro*, only a few literatures have been made on *in vivo* trafficking or monitoring of transplanted stem cells in MI. Initial imaging studies on fusion of ^{18}F-FDG and ^{18}F-FHBG 9-(4-^{18}F-fluoro-3-(hydroxymethyl)butyl)guanine (^{18}F-FHBG) imaging allowed identification of ESCs at 2 weeks after transplantation*(1)*, and ^{18}F-FHBG PET combined with MR imaging presented excellent detection of double labeling of ESCs with *HSV1-sr39tk* reporter gene and superparamagnetic iron oxide particlesfor up to 4 weeks in MI rats*(2)*. Recently, several studies have reported the uses of iPSC-CMs in providing functional benefit after MI, although there has been no consensus about the protective mechanism induced by these differentiated cardiomyocytes *(11)*. By using cardiac MRI and compared to the non-treated PBS control, Wu JC and his colleagues *(12)* found that iPSC-CMs promoted cardiac protection and attenuated cardiac remodeling after MI, despite of limited engraftment detected with bioluminescence imaging. In our present study, we found that iPSCs and iPSC-CMs group demonstrated steadily increasing of ^{18}F-FDG accumulation during the 4-week period, whereas the ESCs group showed higher accumulation only in the earlier stage, indicating that iPSCs, especially the iPSC-CMs may produce a more stable therapeutic response than that of the ESCs or ESC-CMs.

Furthermore, our serial immunofluorescent analysis (with 5 time points), transplanted stem cells survived and migrated to the peri-infarct area, expressed the markers of myocardial (cTNI and cTNT), endothelial (vWF), and smooth muscle or myofibroblast cells (α-SMA). This observations suggested that the metabolic and functional recovery after stem cell transplantation might due to transplanted cells differentiating into myocardial cells, secreting paracrine factors, or recruiting peripheral stem cells to the ischemic territory *(11)*. Interestingly, a very recent study *(13)* found that hESC-derived myocardial precursors (hMPs) treatment resulted in improvement of cardiac function with smaller infarct size and less wall thinning, induced endogenous angiogenesis with increased capillary density, and reduced apoptosis of host cardiomyocytes as the peri-infarct area within 4 weeks post-MI in mice *(13)*.

Unfortunately, their staining has been done for only two time points. In contrast, our serial immunofluorescent staining provided a full-time course after stem cell transplantation post-MI, which demonstrated more cells with $cTNT^+$, vWF^+ and $\alpha\text{-}SMA^+$ at the earlier stages compared to the later ones.

CONCLUSION

Serial ^{18}F-FDG PET and echocardiographic imaging studies demonstrated the dynamic metabolic changes and myocardial functional recovery after stem cell transplantation. ^{18}F-FDG PET could be a potential approach to evaluate the *in vivo* spatiotemporal dynamic metabolic changes post iPSCs or iPSC-CMs transplantation after ischemic injury.

ACKNOWLEDGMENT

We thank Drs. Zhi Jiang, Han Chen for their excellent technical support. This work is supported by grants from the National Science Foundation of China (NSFC) (No. 81170306), Science Technology Program of Zhejiang Province (2012C13013-2), National Major Research Program of China (2016YFA0100900) and the Fundamental Research Funds for the Central Universities of China (2013QNA7021).

REFERENCES

1. Cao F, Lin S, Xie X, et al. In vivo visualization of embryonic stem cell survival, proliferation, and migration after cardiac delivery. Circulation. 2006;113(7):1005-14.
2. Qiao H, Zhang H, Zheng Y, et al. Embryonic stem cell grafting in normal and infarcted myocardium: serial assessment with MR imaging and PET dual detection. Radiology. 2009;250(3):821-9.
3. Carpenter L, Carr C, Yang CT, et al. Efficient differentiation of human induced pluripotent stem cells generates cardiac cells that provide protection following myocardial infarction in the rat. Stem Cells Dev. 2012;21(6):977-86.
4. Lang C, Lehner S, Todica A, et al. Positron emission tomography based in-vivo imaging of early phase stem cell retention after intramyocardial delivery in the mouse model. Eur J Nucl Med Mol Imaging. 2013;40(11):1730-8.
5. Kawamura M, Miyagawa S, Miki K, et al. Feasibility, safety, and therapeutic efficacy of human induced pluripotent stem cell-derived cardiomyocyte sheets in a porcine ischemic cardiomyopathy model. Circulation. 2012;126(11 Suppl 1):S29-S37.
6. Zhang Y, Ruel M, Beanlands RS, et al. Tracking stem cell therapy in the myocardium: applications of positron emission tomography. Curr Pharm Des. 2008;14(36):3835-53.
7. Jiang H, Cheng Z, Tian M, Zhang H. In vivo imaging of embryonic stem cell therapy. Eur J Nucl Med Mol Imaging. 2011;38(4):774-84.
8. Masumoto H, Matsuo T, Yamamizu K, et al. Pluripotent stem cell-engineered cell sheets reassembled with defined cardiovascular populations ameliorate reduction in infarct heart function through cardiomyocyte-mediated neovascularization. Stem Cells. 2012;30(6):1196-205.
9. Takahashi K, Yamanaka S. Induction of pluripotent stem cells from mouse embryonic and adult fibroblast cultures by defined factors. Cell. 2006;126(4):663-76.
10. Perin EC, Tian M, Marini FC, et al. Imaging long-term fate of intramyocardially implanted mesenchymal stem cells in a porcine myocardial infarction model. PLoS One. 2011;6(9):e22949.
11. Lalit PA, Hei DJ, Raval AN, Kamp TJ. Induced pluripotent stem cells for post-myocardial infarction repair: remarkable opportunities and challenges. Circ Res. 2014;114(8):1328-45.
12. Ong SG, Huber BC, Hee Lee W, et al. Microfluidic Single-Cell Analysis of Transplanted Human Induced Pluripotent Stem Cell-Derived Cardiomyocytes After Acute Myocardial Infarction. Circulation. 2015;132(8):762-71.
13. Ye J, Gaur M, Zhang Y, et al. Treatment with hESC-Derived Myocardial Precursors Improves Cardiac Function after a Myocardial Infarction. PLoS One. 2015;10(7):e0131123.

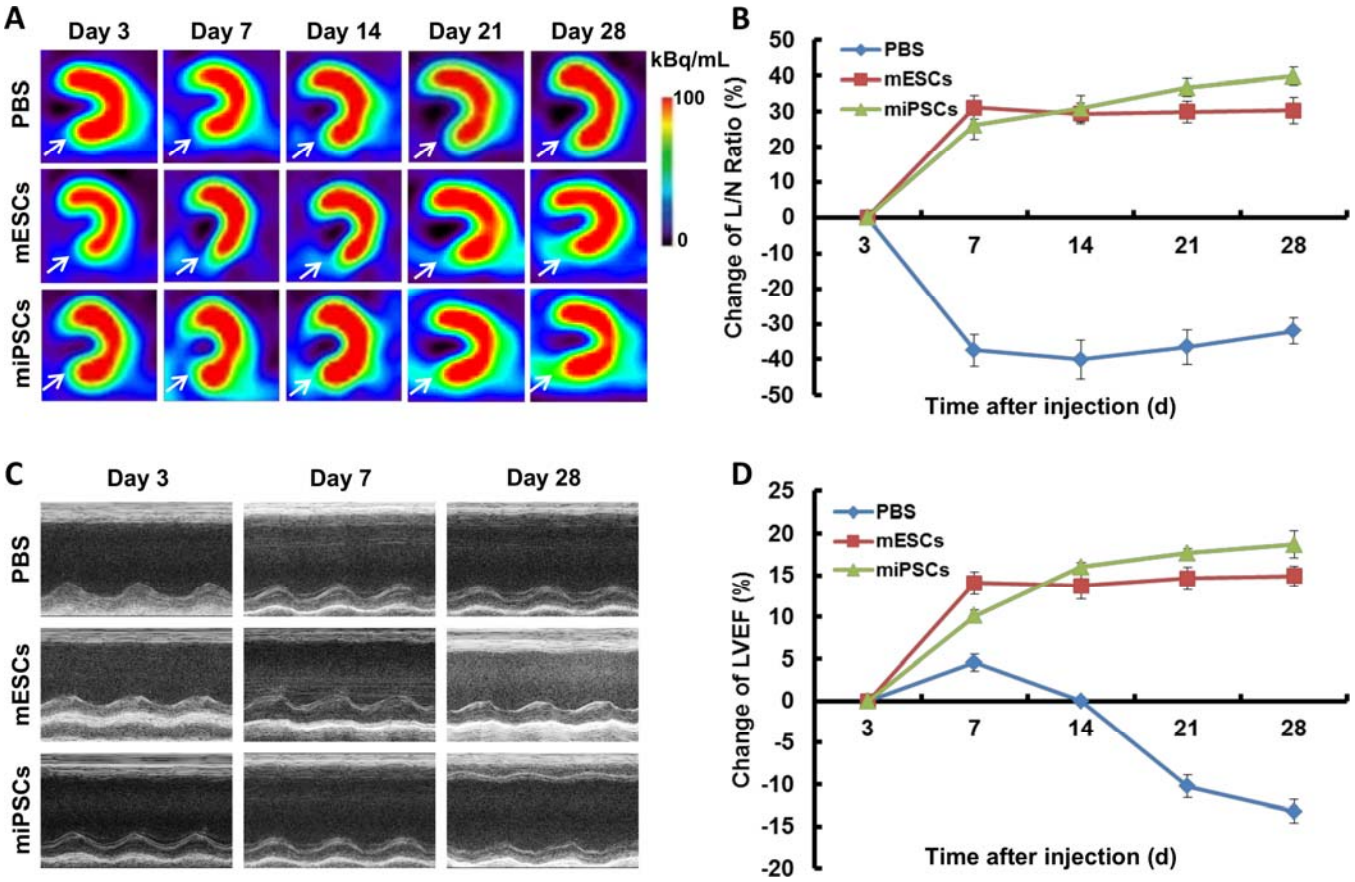

Figure 1. Serial PET and echocardiographic studies after miPSCs and mESCs transplantation compared to the PBS control in a rat model of MI. (A) Representative PET images demonstrating better metabolic recovery after stem cell transplantation (*white arrows*). Images are shown in axial view. Scale was set according to signal intensity. (B) Semi-quantitative analysis of change of L/N ratio demonstrating significant increase of glucose metabolism in the miPSCs and mESCs groups compared to the PBS control ($P < 0.05$). (C) Representative M-mode echocardiographic images and (D) LVEF analysis demonstrating significant cardiac functional improvement after miPSCs and mESCs transplantation compared to the PBS control ($P < 0.05$).

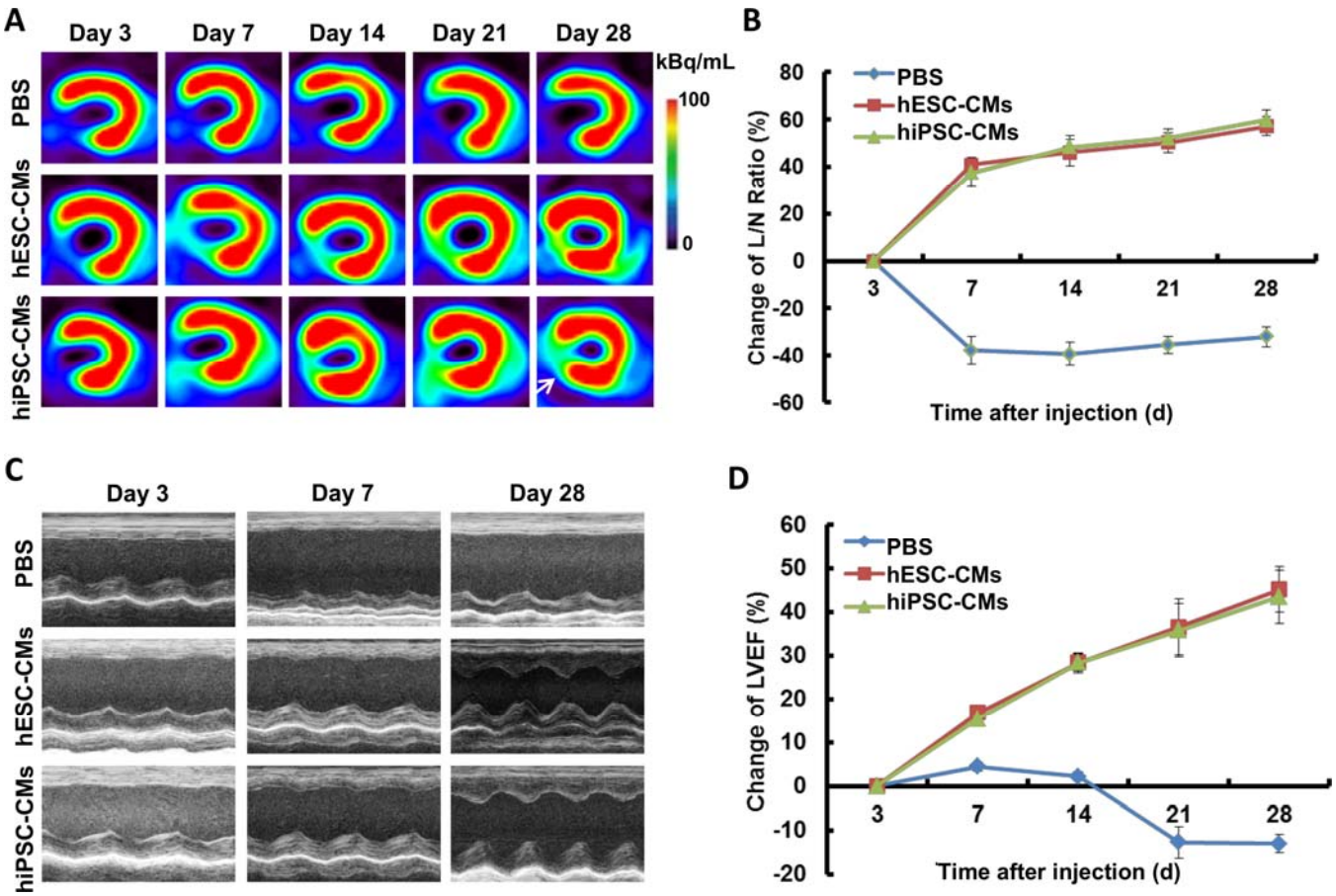

Figure2. Serial PET and echocardiographic studies after hiPSC-CMs and hESC-CMs transplantation compared to the PBS control in a rat model of MI. (A) Representative PET images demonstrating better metabolic recovery after hiPSC-CMs and hESC-CMs transplantation (white arrows). Images are shown in axial view. Scale was set according to signal intensity. (B) Semi-quantitative analysis of change of L/N ratio demonstrating significant increase of glucose metabolism in the hiPSC-CMs and hESC-CMs groups compared to the PBS control ($P < 0.05$). (C) Representative M-mode echocardiographic images and (D) LVEF analysis demonstrating significant cardiac functional improvement after hiPSC-CMs and hESC-CMs transplantation compared to the PBS control ($P < 0.05$).

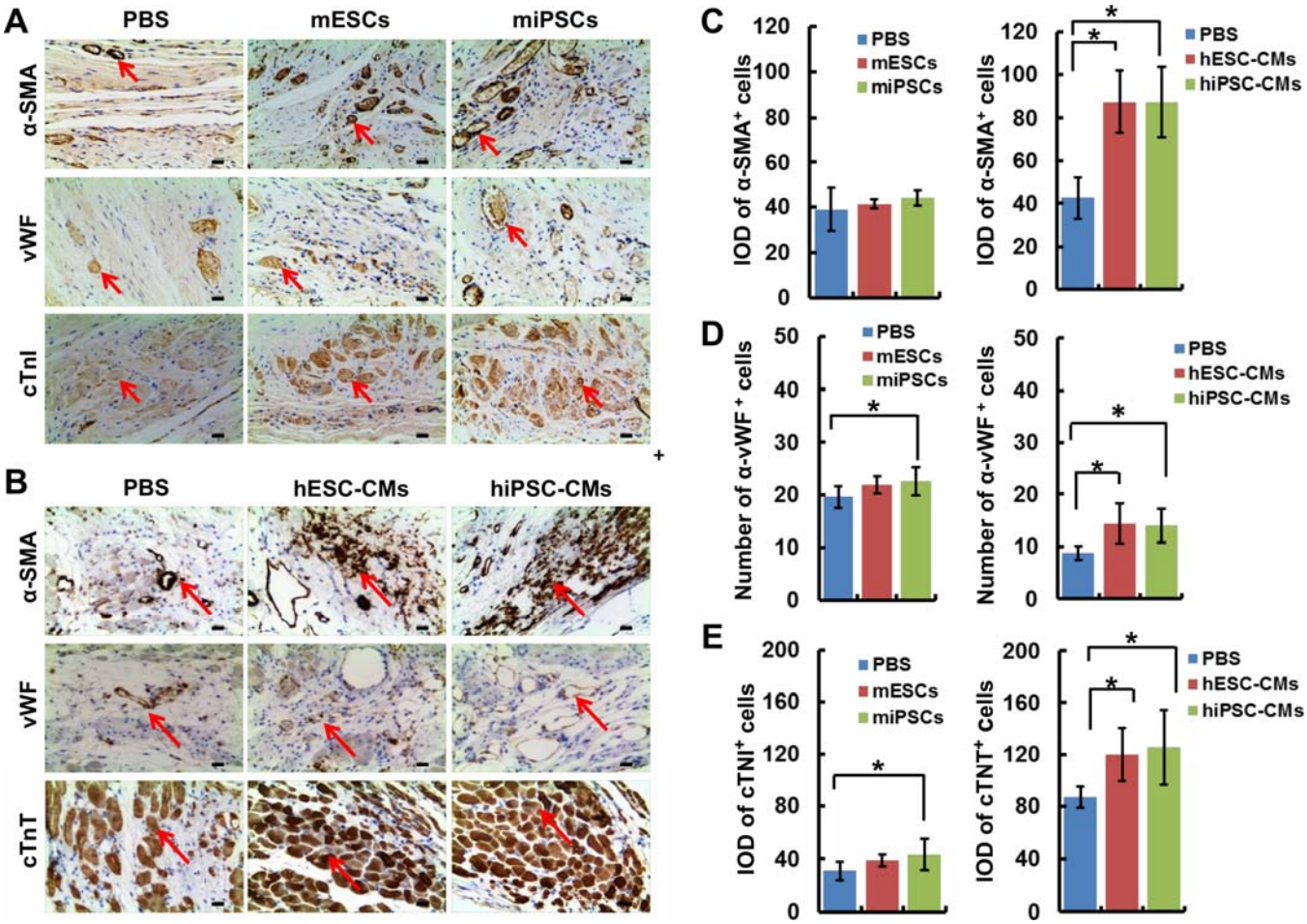

Fig. 3 Immunohistochemical staining of α-SMA, vWF, cTnI and cTnT (*red arrows*). (A) Representative images of ischemic region in miPSCs and mESCs or PBS-injected rats. (B) Representative images of ischemic region in hiPSC-CMs and hESC-CMs or PBS-injected rats. Scale bar = 50 μm. (C) a-SMA-positive cells. *P < 0.05, compared with the PBS control. (D) vWF-positive cells. *P< 0.05, compared with the PBS control. (E) cTnI and cTnT - positive cells. *P < 0.05, compared with PBS control.